Developing apatites for solid oxide fuel cells: insight into structural, transport and doping properties†

Emma Kendrick,[a] M. Saiful Islam[b] and Peter R. Slater*[a]

Received 23rd March 2007, Accepted 21st May 2007
First published as an Advance Article on the web 7th June 2007
DOI: 10.1039/b704426g

Materials displaying high oxide-ion conductivity have attracted considerable interest due to technological applications in solid oxide fuel cells (SOFCs), oxygen sensors and separation membranes. This has driven research into the identification of new classes of oxide-ion conductors, and in this review, work on the recently discovered apatite-type silicate/germanate oxide-ion conductors is presented. In contrast to the traditional perovskite- and fluorite-based oxide-ion conductors, in which conduction proceeds *via* oxygen vacancies, the research on these apatite systems suggests that the conductivity involves interstitial oxide-ions. In addition, the flexibility of the tetrahedral (Si/GeO_4) framework also plays a crucial role in facilitating oxide-ion migration. Detailed doping studies have shown that the apatite structure is able to accommodate a large range of dopants (in terms of both size and charge state), and the influence of these dopants on the conductivity is discussed.

1. Introduction

Oxide-ion conductors are an important class of materials that form the basis of a range of environmentally-friendly applications such as solid oxide fuel cells (SOFCs), oxygen sensors and oxygen separation membranes. In terms of clean energy conversion to decrease the level of carbon emissions, there is considerable interest in SOFC devices as their high efficiency and ability to act as a bridging technology between hydrocarbon and hydrogen fuel systems make them major candidates for next generation power production.[1,2]

The conventional SOFC electrolyte material is yttria-stabilised zirconia (YSZ), although very high temperatures of about 1000 °C are required in order to achieve sufficient oxide-ion conductivity. There is, therefore, considerable interest in developing alternative electrolytes with lower operating temperatures ideally in the range 600–700 °C. A variety of materials are being investigated for so-called intermediate-temperature SOFCs, with research dominated by fluorite-type oxides (such as Gd doped CeO_2 and rare-earth doped bismuth oxides), and perovskite-type oxides (such as doped $LaGaO_3$, and Y-doped $BaCeO_3$).[2,3]

Recently, however, a range of rare-earth apatite materials have been proposed as alternative solid electrolyte materials following the exciting discovery of fast oxide-ion conductivity in the silicate-based systems.[4–20] Isostructural with the well-known apatite minerals and hydroxyapatite biomaterials,[21] these materials have the general formula $M_{10}(XO_4)_6O_{2\pm y}$, where M is a metal such as a rare-earth or alkaline earth, and X is a p-block element such as P, Si or Ge. Traditionally their structure has been described as comprising of isolated XO_4 tetrahedra arranged so as to form distinct oxide-ion and M channels running parallel to the *c* axis, the oxide-ion channels being central to the oxide ion conductivity (Fig. 1). An alternative description, proposed by Baikie *et al.*, is as a "microporous" framework ($M_4(XO_4)_6$) composed of face sharing MO_6 trigonal prismatic columns, that are corner connected to the XO_4 tetrahedra (Fig. 2).[22] This framework allows some flexibility to accommodate the remaining $M_6O_{2\pm y}$ units.

A number of rare-earth apatite systems have been synthesized, and it is the lanthanum silicate and germanate analogues that have been found to demonstrate the highest conductivities.[4,5] The carrier species is purely anionic for most compositions, with high oxygen transference numbers ($t_O > 0.9$) across a wide range of oxygen partial pressures.[4,13] The conductivities are comparable to other electrolytes currently being investigated for SOFC applications, with exceptionally high conductivities parallel to the *c* axis reported for single crystals (Fig. 3).

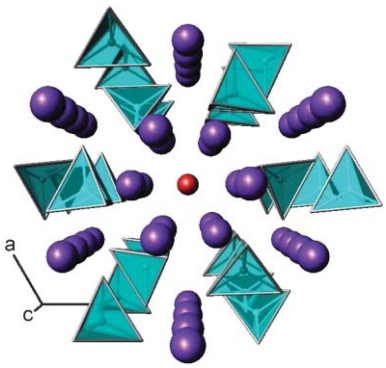

Fig. 1 The apatite structure, $M_{10}(XO_4)_6O_{2\pm y}$, (tetrahedra = XO_4, purple spheres = M, red spheres = O).

[a]*Materials Chemistry Group, Chemistry, SBMS, University of Surrey, Guildford, Surrey, UK GU2 7XH. E-mail: p.slater@surrey.ac.uk; Fax: +44 (0)1483 686851; Tel: +44 (0)1483 686847*
[b]*Department of Chemistry, University of Bath, Bath, UK BA2 7AY*
† This paper is part of a *Journal of Materials Chemistry* theme issue on New Energy Materials. Guest editor: M. Saiful Islam.

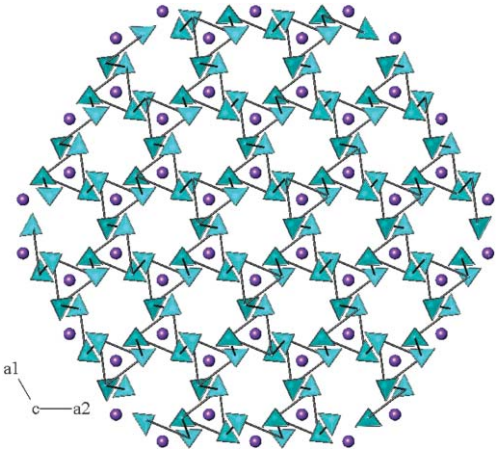

Fig. 2 Alternative representation of the apatite structure: illustration of the "microporous" $M_4(XO_4)_6$ framework. The cavities are where the remaining $M_6O_{2\pm y}$ units would occupy.

It is found that these materials are tolerant to an unusually broad range of dopants, particularly on the rare-earth sites, with the observed conductivity being very sensitive to the doping regime and cation–anion non-stoichiometry.[4–13] The highest conductivities are, however, found for the oxygen-excess samples, and it has thus been suggested that interstitial oxide-ion conduction occurs along the oxide-ion channels.

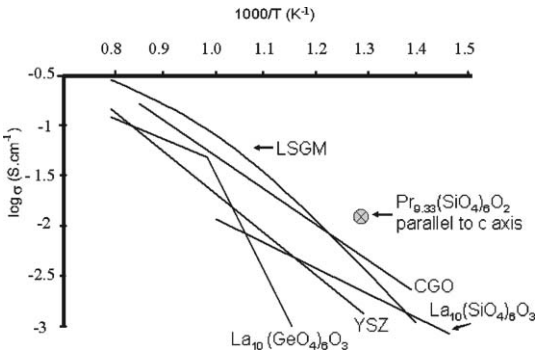

Fig. 3 Comparison of conductivity data for selected oxide-ion conductors (LSGM = $La_{0.9}Sr_{0.1}Ga_{0.8}Mg_{0.2}O_{2.85}$, YSZ = $Y_{0.15}Zr_{0.85}O_{1.925}$, CGO = $Ce_{0.9}Gd_{0.1}O_{2-x}$) with those from initial reports for apatite conductivities.[4,23] Data point for $Pr_{9.33}(SiO_4)_6O_2$ single crystal parallel to *c* axis[24] shown to emphasise exceptionally high *c* axis oxide-ion conductivity in these apatite systems.

This review focuses on the state of our present knowledge and recent progress in the investigation of these fascinating Si- and Ge-based apatite materials, $Ln_{9.33+x}(Si/GeO_4)_6O_{2+3x/2}$ (Ln = rare earth), which form a new family of oxide-ion conductors. A variety of techniques, including high resolution neutron diffraction, atomistic computer modelling and Si-NMR, have assisted in providing fresh insight into these complex oxides. The following sections provide a current survey of synthesis, conductivity, modelling and doping studies of Si- and Ge-based apatite systems. We highlight fundamental work on probing their bulk and local structures, ion conduction mechanisms and cation doping effects that underpin the greater understanding of their macroscopic behaviour and the ability to optimise their transport parameters for potential clean energy applications.

2. Si-Based systems: $Ln_{9.33+x}(SiO_4)_6O_{2+3x/2}$

2.1 Synthesis methods

Following the initial reports by Nakayama *et al.* of high oxide-ion conductivity in $Ln_{9.33+x}(SiO_4)_6O_{2+3x/2}$,[4] there have been a

M. Saiful Islam

Prof. Saiful Islam studied at University College London, completing his PhD in 1987 with Professor Richard Catlow FRS. He then held a Postdoctoral Fellowship at the Eastman Kodak Labs in Rochester, New York, USA. Saiful returned to the UK to become Lecturer and then Reader at the University of Surrey. In early 2006 he was appointed Professor of Computational Materials Chemistry at the University of Bath. Saiful's interests lie in the field of inorganic solid-state chemistry, focusing on atomistic modelling and structural studies of oxide materials for fuel cells and lithium-ion batteries.

Emma Kendrick

Dr Emma Kendrick is a Research Fellow at the University of Surrey. She has a background in solid state chemistry, covering the development of low temperature synthesis routes and structural chemistry. Present research has focused on the use of combined experimental and modelling studies to elucidate the conduction mechanisms of novel ionic conductors.

Peter R. Slater

Dr Peter Slater is a Senior Lecturer at the University of Surrey. His research background is in solid state chemistry, including solid oxide fuel cells, high temperature superconductivity, fast ion conductors, and structural studies of inorganic solids. His present research is focusing mainly on the development of novel ionic and mixed conductors for energy storage and conversion applications.

number of reports on optimising the synthesis of these systems. Single crystal samples have been prepared by the floating zone method,[25] while studies on polycrystalline samples initially concentrated on the use of the standard solid state synthesis route.[4,7–10] Although successful in the preparation of high quality samples, the solid state reaction route requires high temperature treatments (typically >1300 °C) to achieve single phase samples. Furthermore, in order to produce dense membranes *via* this route for potential applications, *e.g.* as SOFC electrolytes, even higher temperatures (typically >1600 °C) are required. Consequently there is growing interest in the optimisation of lower temperature synthesis methods, and in this respect sol–gel routes have been attracting significant attention.[5,18,19] Such routes have typically involved the use of alkoxide precursors, with synthesis temperatures as low as 800 °C being reported, along with a reduction in the sintering temperature by up to 300 °C. More recently Rodriguez-Reyna *et al.* have reported the synthesis of these systems by mechanically milling the constituent oxides at room temperature.[26] The formation of the apatite phase was shown to proceed fastest with the use of amorphous SiO_2.

2.2. Relationship between composition and conductivity

The initial work by Nakayama *et al.* on undoped $Ln_{9.33+x}(SiO_4)_6O_{2+3x/2}$ showed that the highest oxide-ion conductivities were observed for the larger rare earths, La, Pr, and Nd.[4,27] Moreover the conductivities were shown to be enhanced in samples containing oxygen excess ($x > 0$), (*e.g.* σ (500 °C) = 1.1 × 10^{-4} S cm^{-1} for $La_{9.33}(SiO_4)_6O_2$, *versus* 1.3 × 10^{-3} S cm^{-1} for $La_{9.67}(SiO_4)_6O_{2.5}$).[8] These initial results suggested that interstitial oxide-ions were important in promoting high oxide-ion conductivity in these apatite systems. Typically non-stoichiometry ranges of $0 \leqslant x \leqslant 0.34$ are possible for the larger rare earths before impurities such as Ln_2SiO_5 appear. For the smaller rare earths, *e.g.* Gd, lower non-stoichiometry ranges are observed, which suggests less space is available to accommodate the extra interstitial oxide-ions as the unit cell size is reduced. In addition a general decrease in conductivity and increase in activation energy is observed as the size of the rare earth is reduced.

In order to identify strategies for the optimisation of the conductivities, a wide range of doping studies have been performed, with the majority of work focusing on the La containing system, $La_{9.33+x}(SiO_4)_6O_{2+3x/2}$, due to the higher conductivities of this system in comparison to samples containing smaller rare earths.

This work has shown that there is a wide range of successful doping possibilities, in addition to the possibility of varying the rare earth, as listed below (along with the dopant site).[8–10,13,15,17,28,29]

La site: Mg, Ca, Sr, Ba, Co, Ni, Cu, Mn, Bi.

Si site: B, Al, Ga, Zn, Mg, Ti, Ge, Fe, Co, Ni, Cu, Mn, P.

A number of dopants (Mg, Mn, Ni, Cu, Co) have been found to be capable of substituting onto either the La or the Si site. Due to the dual site possibilities of these dopants, we have termed them "ambi-site" dopants. For the transition metal cations, there is evidence that the charge on the dopant ion is dictated by the host lattice site; for example XANES studies have shown that Co will substitute onto the La site as Co^{2+}, but onto the Si site as Co^{3+}.[15] The results from these doping studies are consistent with dopant incorporation trends determined from modelling studies, which predict that larger dopants favour the La site, while smaller dopants favour the Si site, with the possibility for ambi-site substitution at intermediate sizes.[30] These results emphasise the flexibility of the apatite structure, allowing the accommodation of dopants covering a wide range of ionic radii (from Ba^{2+} to Mg^{2+} for the La site, and from B^{3+} to Mg^{2+} on the Si site). This structural flexibility can be readily seen by examining the local relaxation around the dopant ion, with modelling studies showing that local distortions and alteration of site sizes are readily possible.[30] In particular, small dopants (*e.g.* Mg^{2+}) are accommodated on the La site furthest from the oxide-ion channels by a change in site coordination from 9 to 6, giving a more ideal coordination for the dopant ion.[17,30]

The doping studies have provided further evidence of the importance of interstitial oxide-ions in these systems. Initial doping studies focused on alkaline earth substitutions and such studies showed that, as the alkaline earth content increased and hence the number of cation vacancies decreased, the conductivity decreased, with the conductivity of the fully stoichiometric materials, $La_8M_2(SiO_4)_6O_2$ (M = Ca, Sr, Ba) being very low (*e.g.* σ (800 °C) = 5.6 × 10^{-7} S cm^{-1} for $La_8Sr_2(SiO_4)_6O_2$). In contrast, alkaline earth doped samples containing oxygen excess, *e.g.* $La_9M(SiO_4)_6O_{2.5}$ (M = Ca, Sr, Ba), all exhibited high oxide-ion conductivities.[8] These systems, which are cation stoichiometric but contain an oxygen excess, showed very high (>10^{-3} S cm^{-1} at 500 °C) conductivities with values comparable to that of equivalent samples containing both cation vacancies and oxygen excess, *e.g.* $La_{9.67}(SiO_4)_6O_{2.5}$.

Doping with aliovalent cations on the Si site has provided some further interesting results, with a significantly different effect on the conductivity *versus* the La site, for samples stoichiometric in oxygen. For these samples, the results show that substituting low levels of lower valent dopants on the Si site tends to enhance the conductivity while a similar doping strategy on the La site tends to result in a decrease in conductivity.[8–10,28,29] The magnitude of the observed change in conductivity is strongly dependent on the size of the dopant cation, with small dopants (*e.g.* Mg) on the La site being particularly detrimental to the conductivity. This behaviour is more clearly visualised by plotting conductivity data for oxygen stoichiometric samples with the same level of cation vacancies but with different dopants (Fig. 4); the difference is particularly dramatic for Mg, which is an ambi-site dopant. The origin of the decrease in conductivity on doping small cations on the La site has been attributed to the effect of the coordination environment being reduced from 9 (for La) to 6 (for small cations, *e.g.* Mg) coordination, and its consequent influence on the oxide ion channels.[17] The detrimental effect of small cation dopants on the La site also extends to samples containing oxygen excess, as can be seen from Fig. 5, which shows conductivity data for selected samples with the same excess oxygen content.

In terms of isovalent dopants, Ge (for Si) doping leads to high conductivities,[9] while Ti (for Si) and Bi (for La) doping

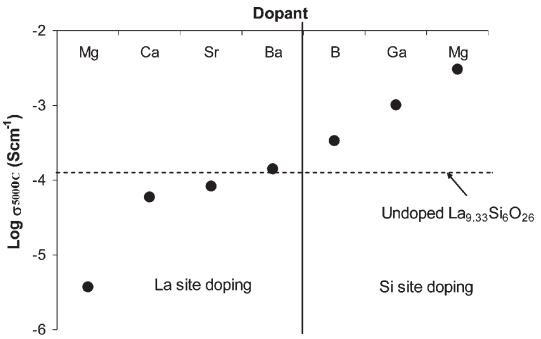

Fig. 4 Comparison of the conductivities (500 °C) of oxygen stoichiometric samples with the same level of cation vacancies, but with differing dopants. Compositions = $La_{9.67}(SiO_4)_5(MO_4)O_2$ (M = B, Ga), $La_{9.67}(SiO_4)_{5.5}(MgO_4)_{0.5}O_2$, $La_{8.67}M(SiO_4)_6O_2$ (M = Mg, Ca, Sr, Ba).

have been shown to dramatically decrease the conductivity; thus the conductivities of $La_9Ba(SiO_4)_4(TiO_4)_2O_{2.5}$ and $La_7BaBi_2(SiO_4)_6O_{2.5}$ are respectively 4 and 3 orders of magnitude lower than that of $La_9Ba(SiO_4)_6O_{2.5}$ at 500 °C (Fig. 5).[9,13] In the case of Ti doping, it has been suggested that this is due to trapping of the interstitial oxygens by Ti increasing its coordination sphere.[9] The origin of the reduction in conductivity for the Bi doped samples requires further study, but may be related to the influence of the Bi lone pair. In this respect, Pb containing apatites (*e.g.* $Pb_8K_2(PO_4)_6$) containing no channel anions have been reported in the literature, and it has been proposed that the lone pair of Pb^{2+} occupies the vacant channel space.[31] Therefore, if the lone pair on the Bi similarly encroaches the oxide-ion channels, then a partial blocking of the conduction pathway may be envisaged.

These detailed conductivity studies, identifying the very high conductivities of samples containing oxygen excess, provide clear support for the importance of interstitial oxide-ions. It was initially unclear, however, why samples which were oxygen stoichiometric, but contained cation vacancies, also showed high conductivities. To account for this feature, neutron powder diffraction structural studies and atomistic simulation studies have been performed. This multi-technique approach has suggested that the presence of cation vacancies increases the oxide-ion interstitial concentration, through the promotion of the formation of Frenkel defects.[7,20]

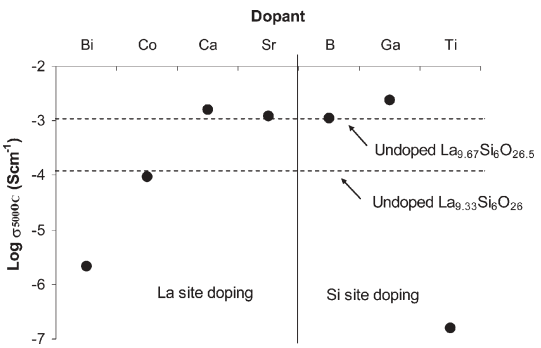

Fig. 5 Comparison of the conductivities (500 °C) of samples with the same level of oxygen excess, but with differing dopants. Compositions = $La_7BaBi_2(SiO_4)_6O_{2.5}$, $La_{9.4}Co_{0.4}(SiO_4)_6O_{2.5}$, $La_9M(SiO_4)_6O_{2.5}$ (M = Ca, Sr), $La_{10}(SiO_4)_5(MO_4)O_{2.5}$ (M = B, Ga), $La_9Ba(SiO_4)_4(TiO_4)_2O_{2.5}$.

2.3 Modelling studies: interstitial site and conduction pathway

As detailed above, the experimental work indicated the importance of interstitial oxide-ions. It was initially believed that these were located down the centre of the oxide-ion channels, a feature apparently supported by the high anisotropic thermal displacement parameter (U_{33}) for the channel oxygen in this direction.[7] However it must be considered that this site lies upon a 6-fold rotation axis, with the thermal displacement parameters consequently constrained by symmetry. Consequently *any* disorder along *c* will be accommodated by U_{33}, not just disorder along the (0,0,*z*) channel centre, meaning that displacements along *x*,*y* are difficult to assess. An additional feature from the structural studies was the similarly high thermal displacement parameters for the silicate unit oxygen atoms. This implies significant local structural distortions around these sites, and a possible contributing factor in the conduction process for these sites.

In order to investigate the conduction mechanism in more detail, atomistic modelling studies were performed on the two systems, $La_{9.33}(SiO_4)_6O_2$ and $La_8Sr_2(SiO_4)_6O_2$, the former showing high conductivity while the latter is a poor oxide-ion conductor.[20] A principal result of this work was the location of a new energetically favourable oxygen interstitial site (Fig. 6). This interstitial oxygen, rather than being located down the channel centre, as initially thought, was accommodated at the channel periphery. The position is stabilised by the displacement of the nearby silicate unit towards the La channels, accounting for the high thermal displacement parameters observed for the silicate oxygen atoms. Subsequently the predicted location of this channel periphery site was confirmed by further structural studies of oxygen excess $La_{9.33+x}(Si/GeO_4)_6O_{2+3x/2}$.[12] Additional support for this interstitial oxide-ion site has come from ^{29}Si NMR studies of a range of alkaline earth doped apatite silicates.[16] These studies have shown a correlation between the ^{29}Si NMR spectra and the conductivity, with poorly conducting samples demonstrating a single NMR resonance, whereas in fast ion conducting compositions, an extra peak was apparent, attributed to a silicate group adjacent to an interstitial oxygen site. This can be seen in Fig. 7, with the poorly conducting $La_8Ba_2(SiO_4)_6O_2$ having a single NMR peak, consistent with a single Si

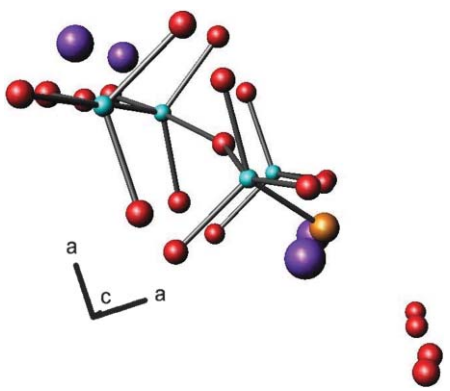

Fig. 6 The interstitial oxygen site (orange sphere) at the periphery of the channels, and associated lattice relaxation (purple spheres = La, blue spheres = Si).

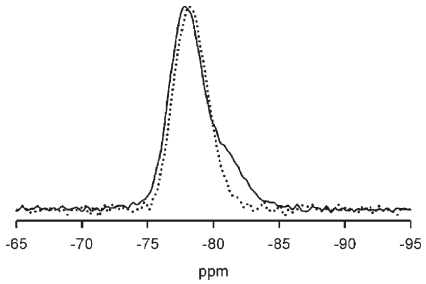

Fig. 7 ^{29}Si NMR spectra for $La_8Ba_2(SiO_4)_6O_2$ (dotted line) and $La_9Ba(SiO_4)_6O_{2.5}$ (full line) showing the presence of a second peak for the latter phase.

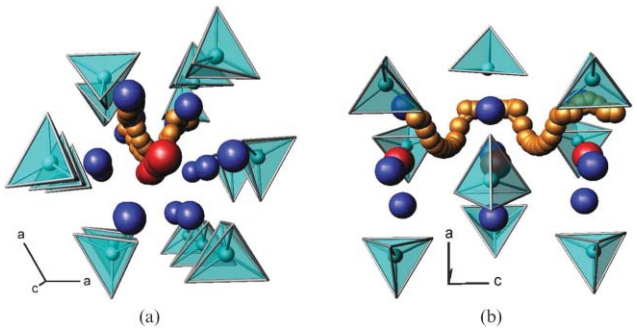

Fig. 8 Interstitial oxide-ion migration pathway in $La_{9.33}(SiO_4)_6O_2$ from atomistic simulation studies; (a) view down the *c* axis; (b) view perpendicular to the *c* axis.

environment, while the highly conducting $La_9Ba(SiO_4)_6O_{2.5}$ has a second peak.

In addition to identifying the position of the most favourable interstitial site, the atomistic simulation studies were also used to examine possible conduction models including both vacancy and interstitial migration. These results suggested that the conduction mechanism in $La_{9.33}(SiO_4)_6O_2$ is *via* an interstitial mechanism, while that of $La_8Sr_2(SiO_4)_6O_2$ involves a vacancy mechanism,[20] with good correlation between observed and calculated activation energies. The predicted interstitial conduction pathway is a complex sinusoidal process as shown in Fig. 8. An important feature is that the conduction process is aided by cooperative displacements of the silicate substructure, suggesting that the flexibility of the silicate substructure is essential to the observed high oxide-ion conductivities. This result ties in with the high thermal displacement parameters for the silicate oxygen atoms observed in diffraction studies noted earlier, particularly for the oxygen atoms sharing a face with the oxide-ion channel.

In order to gain further information regarding the conduction process, molecular dynamics (MD) simulation studies are planned. In particular, there is a need to investigate the possibility of interstitialcy (knock-on) mechanisms, which are difficult to assess through static lattice simulations. In addition, detailed conductivity studies of single crystals of $Ln_{9.33}(SiO_4)_6O_2$ have thrown up some interesting features, which have largely been overlooked. These studies have shown that the conductivity is anisotropic, with the conductivity parallel to *c* (the direction of the oxygen channels) significantly higher than that perpendicular (*e.g.* $Pr_{9.33}(SiO_4)_6O_2$, $\sigma_c = 1.3 \times 10^{-2}$ S cm^{-1}, $\sigma_{ab} = 1.2 \times 10^{-3}$ S cm^{-1} at 500 °C).[24] Although this appears to support the assumption that the oxygen channels are responsible for the high oxide-ion conductivity, the enhancement along *c* (approximately one order of magnitude) is not as high as might be expected considering the anisotropy of the structure. In addition the activation energies for conduction along *c* and along *a*,*b* are fairly similar ($Pr_{9.33}(SiO_4)_6O_2$; low temperature $E_{act}(c) = 0.68$ eV, $E_{act}(a,b) = 0.62$ eV).[24] These results suggest that although the main conduction pathway is down the oxide-ion channels, there is also significant conduction perpendicular to the channels (*i.e.* inter-channel conduction).

One possible explanation for inter-channel conduction has come from a close inspection of the local structural distortions near an oxide-ion interstitial site from computer modelling studies. This shows that the local relaxation around the interstitial site leads to reduction in the distance to a neighbouring SiO_4 unit. This could effectively create a pathway, whereby an interstitial oxide-ion is moved between adjacent channels by a series of two cooperative "S_N2"-type processes (S_N2 = bimolecular nucleophilic substitution), with accompanying rotation of the tetrahedra (Fig. 9).

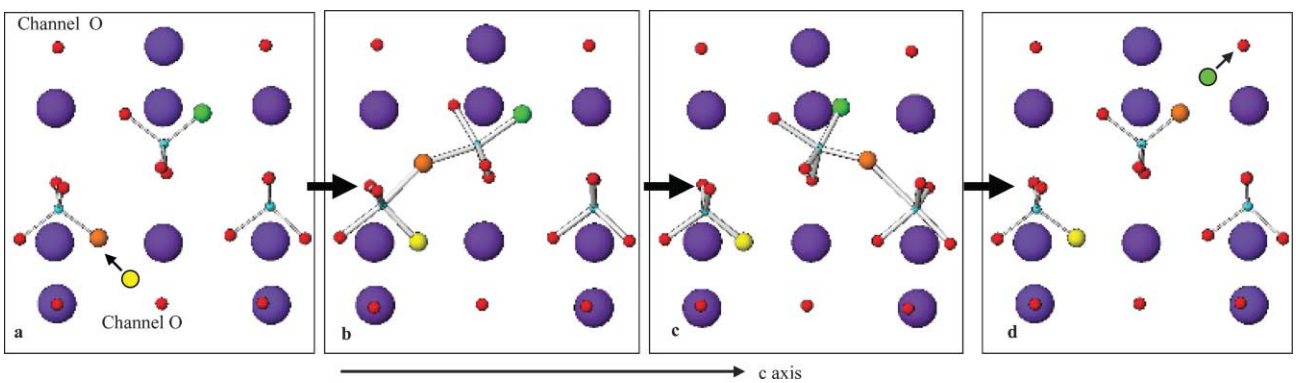

Fig. 9 Proposed conduction pathway between adjacent oxide-ion channels *via* two "S_N2"-type processes, with accompanying rotation of the silicate tetrahedra, obtained from computer simulation results of $La_{9.33}(SiO_4)_6O_2$. The incorporation of a periphery interstitial oxide-ion (yellow) (a) forces a silicate oxygen (orange) in between the two SiO_4 units forming an Si_2O_9 unit (b), the top silicate unit rotates to form an Si_2O_9 unit with a neighbouring silicate unit (c), and an oxygen on the top silicate unit (green) is released as an interstitial in a different channel (d).

3. Ge-Based systems: $Ln_{9.33+x}(GeO_4)_6O_{2+3x/2}$

3.1 Synthesis methods

Following the reports of high oxide-ion conductivity in the silicate apatites, similarly high conductivities were reported for germanium-containing analogues, $La_{9.33+x}(GeO_4)_6O_{2+3x/2}$.[23] The majority of the work on these systems has focused on the standard solid state synthesis route, requiring synthesis temperatures of 1100–1200 °C, and sintering temperatures to achieve dense pellets for conductivity measurements of >1400 °C. The elevated temperatures for the latter, in particular, raises a key problem of Ge volatility.[32–34] This Ge loss leads to an increase in the La : Ge ratio, with La_2GeO_5 impurities being observed on extended high temperature (1500 °C) heating.[32] Therefore the composition of samples will change on sintering at the typical temperatures required to achieve dense membranes. Moreover, the composition will vary across the membrane, with the surface expected to be significantly Ge deficient. Consequently there is a crucial need to lower these temperature requirements through alternative synthesis routes and/or doping studies. In this respect, Rodríguez-Reyna *et al.* have succeeded in synthesising germanate apatites by mechanical milling of the precursor powders.[26] These studies have shown that the synthesis of $La_{9.33+x}(GeO_4)_6O_{2+3x/2}$ can be achieved by room temperature milling of the oxides La_2O_3 and GeO_2 in as little as 6 hours. More recently we have developed a Pechini-type sol–gel process to synthesise these germanate apatites.[35] In this method citric acid and ethylene glycol are added to a solution of lanthanum nitrate and GeO_2, and the resulting mixture is evaporated until gel formation. This route allows the synthesis of pure $La_{9.33+x}(GeO_4)_6O_{2+3x/2}$ at 800 °C, with sintering to produce dense pellets at temperatures of ≈1300 °C.

3.2. Relationship between composition, structure and conductivity

An additional complexity of the germanate apatites is a change in cell symmetry with increasing La content, with a number of important studies in this area.[11,12,22,34,36,37] Leon-Reina *et al.* have reported that the $La_{9.33+x}(GeO_4)_6O_{2+3x/2}$ system can be prepared for $0.19 \leqslant x \leqslant 0.42$, with samples in the range $0.19 \leqslant x \leqslant 0.27$ being shown to have hexagonal symmetry, while samples with higher La content, $0.33 \leqslant x \leqslant 0.42$, exhibit a triclinic cell.[11,12] Detailed neutron diffraction studies of $La_{9.33+x}(GeO_4)_6O_{2+3x/2}$ have identified the presence of interstitial oxide-ion sites at the periphery of the channels in similar positions as for the Si-based systems.

Conductivity studies on $La_{9.33+x}(GeO_4)_6O_{2+3x/2}$ have shown that higher activation energies are observed compared to the analogous silicate systems. As such the low temperature conductivities (<600 °C) tend to be lower than for silicate systems, while the conductivities at higher temperatures are enhanced (Fig. 3). Moreover, high temperature structural studies of triclinic samples have shown that the triclinic cell changes to a hexagonal cell,[34,37] resulting in a corresponding reduction in the activation energy for oxide-ion conduction at elevated temperatures. In addition it has recently been shown that these systems will also incorporate significant amounts of water on annealing in wet atmospheres at temperatures below 500 °C, with evidence for an enhancement in conductivity at low temperatures consistent with a protonic contribution.[37]

As for the silicate systems, it has been shown that it is possible to introduce a wide range of dopants into these germanate apatites. The results have shown that doping with divalent cations (*e.g.* Ba, Sr, Ca, Mg, Cu, Ni, Mn, Co) on the La site helps to stabilise the hexagonal lattice; in contrast, doping on the Ge site (*e.g.* Co, Al, Ga) has a tendency to result in triclinic cells.[9,11,33] The exceptions are B and Ti, which have been shown to substitute on the Ge site, but result in hexagonal cells.[9,33] The complexity of the X-ray diffraction pattern for a triclinic apatite system makes it very difficult to identify small impurity levels, and so further work is required to confirm the solid solution ranges in such cases.

Baikie *et al.* have shown that the driving force for the formation of a triclinic apatite cell rather than a hexagonal cell is the strain introduced by the presence of large cations (*e.g.* Ge, As, V) in the tetrahedral sites.[22] This leads to underbonding (reduced bond valence sum) at the La sites surrounding the oxide-ion channel, which is relieved by the tetrahedral GeO_4 units tilting in the triclinic cell. This accounts for why large dopants on the Ge site, such as Ga, Co have a tendency to produce triclinic systems, as these dopants would be expected to increase this strain.

In terms of the conductivities of these doped systems, samples which are fully stoichiometric, *e.g.* $La_8M_2(GeO_4)_6O_2$ (M = Ca, Sr, Ba), have been shown to have low conductivities, as found for the related Si-based systems; this is consistent with the absence of significant oxide-ion interstitial defects, which has been confirmed by structural studies of $La_8Ba_2(GeO_4)_6O_2$.[33] High conductivities are then observed for samples containing cation vacancies and/or oxygen excess, also in agreement with the results on the silicate systems. There is, however, a significant difference between the silicate and germanate systems in terms of doping effects: in the germanate systems, the conductivities appear to be significantly less influenced by the nature of the dopant or the dopant site. Thus, while the partial substitution of Bi or small cations on the La site, or Ti on the Si site in the silicate systems results in significant decreases in conductivities even for samples containing oxygen excess, such large reductions are not observed for the germanate analogues. Therefore, for the latter, high conductivities (>0.01 S cm^{-1} at 800 °C) are typically observed even for these dopants.

More recently we have shown that the partial substitution of Y for La, *e.g.* $La_{7.33+x}Y_2(GeO_4)_6O_{2+3x/2}$, helps to stabilize the hexagonal lattice even for high levels of x, with high conductivities maintained (*e.g.* $x = 0.34$, σ (800 °C) = 0.035 S cm^{-1}; $x = 0.5$, σ (800 °C) = 0.028 S cm^{-1}). It has also been shown to stabilise the hexagonal lattice for doped samples, *e.g.* $La_8Y_2(GeO_4)_5(CoO_4)O_{2.5}$ (Fig. 10) (σ (800 °C) = 0.027 S cm^{-1}), thus allowing greater ease of identifying dopant incorporation limits. The formation of a hexagonal lattice can be attributed to Y selectively substituting into the $La_4(GeO_4)_6$ framework (Fig. 2), reducing the size of this framework and hence relieving the underbonding at the La sites surrounding the oxide ion channels.

In summary, the doping studies have shown that the conductivities of the germanate systems are less sensitive than

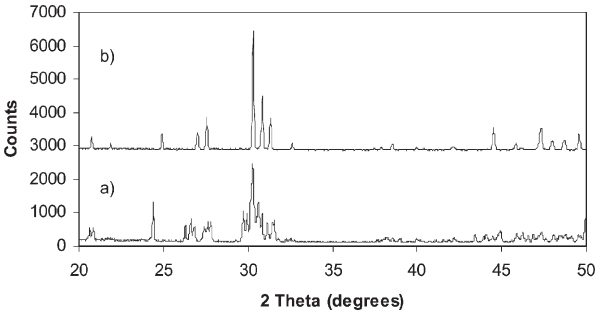

Fig. 10 X-Ray diffraction patterns for (a) $La_{10}(GeO_4)_5(CoO_4)O_{2.5}$ (triclinic cell) and (b) $La_8Y_2(GeO_4)_5(CoO_4)O_{2.5}$ (hexagonal cell).

the silicates to the effect of dopants. This feature is somewhat surprising, and may indicate a range of conduction pathways, making the conductivity less sensitive to localized distortions.

4. Conclusions and outlook

This review has shown that apatite-type materials are a fascinating new family of oxide-ion conductors with potential use in solid oxide fuel cells (SOFCs) and oxygen-permeable membranes.

For high oxide-ion conductivities in the Si- and Ge-based apatites, $Ln_{9.33+x}(Si/GeO_4)_6O_{2+3x/2}$, non-stoichiometry in the form of cation vacancies and/or oxygen excess is required, with the latter giving materials with the highest conductivities. Structural and atomistic modelling studies have indicated that interstitial oxide-ions are the key defect facilitating ion conduction, and that the Si/GeO_4 tetrahedra flexibility also plays a crucial role in the conduction process. This is in contrast to fluorite- and perovskite-type oxides in which oxide-ion conduction proceeds *via* vacancy defect mechanisms. An unusually broad range of dopant ions (in terms of size and charge state) can be incorporated, which is much wider than that observed for doping on a single cation site in most other oxide-ion conductors such as perovskite-type oxides.

Future research will encompass further work on lower temperature synthesis routes, SOFC electrolyte/electrode stability issues, molecular dynamics (MD) simulations of conduction mechanisms and the general search for improved oxide-ion conductors. Indeed, the breadth of possible doping regimes in these apatite materials provides new opportunities to design and optimise their properties for fuel cell electrolytes. The exceptionally high conductivities parallel to the *c* axis reported for $Ln_{9.33}(SiO_4)_6O_2$ single crystals also emphasizes that further enhancements are possible especially if *c* axis orientated membranes can be produced.

Acknowledgements

We would like to thank the EPSRC and The Royal Society for funding.

References

1 (*a*) B. C. H. Steele and A. Heinzel, *Nature*, 2001, **414**, 345; (*b*) A. Atkinson, S. Barnett, R. J. Gorte, J. T. S. Irvine, A. J. McEvoy, M. Mogensen and S. C. Singhal, *Nat. Mater.*, 2004, **3**, 17.
2 (*a*) R. M. Ormerod, *Chem. Soc. Rev.*, 2003, **32**, 17; (*b*) Z. P. Zhou and S. M. Haile, *Nature*, 2004, **431**, 170.
3 (*a*) M. Mamak, G. S. Metraux, S. Petrov, N. Coombs, G. A. Ozin and M. A. Green, *J. Am. Chem. Soc.*, 2003, **125**, 5161; (*b*) S. Tao, J. T. S. Irvine and J. A. Kilner, *Adv. Mater.*, 2005, **17**, 1734.
4 (*a*) S. Nakayama, H. Aono and Y. Sadaoka, *Chem. Lett.*, 1995, 431; (*b*) S. Nakayama, T. Kagayama, H. Aono and Y. Sadoaka, *J. Mater. Chem.*, 1995, **5**, 1801; (*c*) S. Nakayama, Y. Higuchi, Y. Kondo and M. Sakamoto, *Solid State Ionics*, 2004, **170**, 219.
5 S. Tao and J. T. S. Irvine, *Mater. Res. Bull.*, 2001, **36**, 1245.
6 (*a*) H. Yoshioka and S. Tanase, *Solid State Ionics*, 2005, **176**, 2395; (*b*) Y. Masubuchi, M. Higuchi, T. Takeda and S. Kikkawa, *Solid State Ionics*, 2006, **177**, 263.
7 J. E. H. Sansom, D. Richings and P. R. Slater, *Solid State Ionics*, 2001, **139**, 205.
8 (*a*) J. E. H. Sansom, J. R. Tolchard, P. R. Slater and M. S. Islam, *Solid State Ionics*, 2004, **167**, 17; (*b*) A. Najib, J. E. H. Sansom, J. R. Tolchard, P. R. Slater and M. S. Islam, *Dalton Trans.*, 2004, 3106; (*c*) P. R. Slater and J. E. H. Sansom, *Diffus. Defect Data, Pt. B*, 2003, **90–91**, 195; (*d*) J. McFarlane, S. Barth, M. Swaffer, J. E. H. Sansom and P. R. Slater, *Ionics*, 2002, **8**, 149.
9 (*a*) J. E. H. Sansom and P. R. Slater, *Solid State Ionics*, 2004, **167**, 23; (*b*) J. E. H. Sansom, A. Najib and P. R. Slater, *Solid State Ionics*, 2004, **175**, 353; (*c*) J. E. H. Sansom, P. A. Sermon and P. R. Slater, *Solid State Ionics*, 2005, **176**, 1765; (*d*) J. E. H. Sansom, E. Kendrick, J. R. Tolchard, M. S. Islam and P. R. Slater, *J. Solid State Electrochem.*, 2006, **10**, 562.
10 E. J. Abram, D. C. Sinclair and A. R. West, *J. Mater. Chem.*, 2001, **11**, 1978.
11 (*a*) L. León-Reina, M. C. Martín-Sedeño, E. R. Losilla, A. Cabeza, M. Martínez-Lara, S. Bruque, F. M. B. Marques, D. V. Sheptyakov and M. A. G. Aranda, *Chem. Mater.*, 2003, **15**, 2099; (*b*) L. León-Reina, E. R. Losilla, M. Martínez-Lara, S. Bruque, A. Llobet, D. V. Sheptyakov and M. A. G. Aranda, *Chem. Mater.*, 2005, **15**, 2489.
12 L. León-Reina, E. R. Losilla, M. Martínez-Lara, S. Bruque and M. A. G. Aranda, *J. Mater. Chem.*, 2004, **14**, 1142.
13 (*a*) V. V. Kharton, A. L. Shaula, M. V. Patrakeev, J. C. Waerenborgh, D. P. Rojas, N. P. Vyshatko, E. V. Tsipis, A. A. Yaremchenko and F. M. B. Marques, *J. Electrochem. Soc.*, 2004, **151**, A1236; (*b*) A. L. Shaula, V. V. Kharton and F. M. B. Marques, *J. Solid State Chem.*, 2005, **178**, 2050; (*c*) Y. V. Pivak, V. V. Kharton, A. A. Yaremchenko, S. O. Yakovlev, A. V. Kovalevsky, J. R. Frade and F. M. B. Marques, *J. Eur. Ceram. Soc.*, 2007, **27**, 2445.
14 V. Maisonnueve, E. Leduc, O. Bohnke and M. Leblanc, *Chem. Mater.*, 2004, **16**, 5220.
15 J. R. Tolchard, J. E. H. Sansom, M. S. Islam and P. R. Slater, *Dalton Trans.*, 2005, 1273.
16 J. E. H. Sansom, J. R. Tolchard, M. S. Islam, D. Apperley and P. R. Slater, *J. Mater. Chem.*, 2006, **16**, 1410.
17 E. Kendrick, J. R. Tolchard, J. E. H. Sansom, M. S. Islam and P. R. Slater, *Faraday Discuss.*, 2007, **134**, 181.
18 (*a*) S. Celerier, C. Laberty-Robert, J. W. Long, K. A. Pettigrew, R. M. Stroud, D. R. Rolison, F. Ansart and P. Stevens, *Adv. Mater.*, 2006, **18**, 615; (*b*) S. Celerier, C. Laberty-Robert, F. Ansart, P. Lenormand and P. Stevens, *Ceram. Int.*, 2006, **22**, 881.
19 (*a*) Y. Masubuchi, M. Higuchi, T. Takeda and S. Kikkawa, *J. Alloys Compd.*, 2006, **408**, 641; (*b*) H. Yoshioka, *J. Alloys Compd.*, 2006, **408**, 649.
20 (*a*) M. S. Islam, J. R. Tolchard and P. R. Slater, *Chem. Commun.*, 2003, 1486; (*b*) J. R. Tolchard, M. S. Islam and P. R. Slater, *J. Mater. Chem.*, 2003, **13**, 1956.
21 (*a*) Q. H. Shi, J. F. Wang, J. P. Zhang, J. Fan and G. D. Stucky, *Adv. Mater.*, 2006, **18**, 1038; (*b*) J. H. Zhan, Y. H. Tseng, J. C. C. Chan and C. Y. Mou, *Adv. Funct. Mater.*, 2005, **15**, 2005; (*c*) G. He, T. Dahl, A. Veis and A. George, *Nat. Mater.*, 2003, **2**, 552.
22 T. Baikie, P. H. J. Mercier, M. M. Elcombe, J. Y. Kim, Y. Le Page, L. D. Mitchell, T. J. White and P. S. Whitfield, *Acta Crystallogr., Sect. B: Struct. Sci.*, 2007, **63**, 251.
23 (*a*) T. Takeuchi, I. Kondoh, N. Tamari, N. Balakrishnan, K. Nomura, H. Kageyama and Y. Takeda, *J. Electrochem. Soc.*,

2002, **149**, A455; (*b*) T. Ishihara, T. Shibayama, M. Honda, H. Nishiguchi and Y. Takita, *J. Electrochem. Soc.*, 2000, **147**, 1332; (*c*) K. Huang, M. Feng and J. B. Goodenough, *J. Am. Ceram. Soc.*, 1998, **81**, 357; (*d*) H. Arikawa, H. Nishiguchi, T. Ishihara and Y. Takita, *Solid State Ionics*, 2000, **136–137**, 31.
24 (*a*) S. Nakayama, M. Sakamoto, M. Higuchi and K. Kodaira, *J. Mater. Sci. Lett.*, 2000, **19**, 91; (*b*) S. Nakayama and M. Higuchi, *J. Mater. Sci. Lett.*, 2001, **20**, 913.
25 (*a*) M. Higuchi, K. Kodaira and S. Nakayama, *J. Cryst. Growth*, 1999, **207**, 298; (*b*) M. Higuchi, H. Katase, K. Kodaira and S. Nakayama, *J. Cryst. Growth*, 2000, **218**, 282; (*c*) Y. Masubuchi, M. Higuchi, S. Kikkawa, K. Kodaira and S. Nakayama, *Solid State Ionics*, 2004, **175**, 357.
26 (*a*) E. Rodriguez-Reyna, A. F. Fuentes, M. Maczka, J. Hanuza, K. Boulahya and U. Amador, *J. Solid State Chem.*, 2006, **179**, 522; (*b*) E. Rodriguez-Reyna, A. F. Fuentes, M. Maczka, J. Hanuza, K. Boulahya and U. Amador, *Solid State Sci.*, 2006, **8**, 168.
27 S. Nakayama and M. Sakamoto, *J. Eur. Ceram. Soc.*, 1998, **18**, 1413.
28 (*a*) H. Yoshioka and S. Tanase, *Solid State Ionics*, 2005, **176**, 2395; (*b*) H. Yoshioka, *Chem. Lett.*, 2004, **33**, 392.
29 E. Kendrick, M. S. Islam and P. R. Slater, *Solid State Ionics*, 2007, **177**, 3411.
30 J. R. Tolchard, P. R. Slater and M. S. Islam, *Adv. Funct. Mater.*, 2007, **17**, DOI: 10.1012/adfm.200600789.
31 M. Mathew, W. E. Brown, M. Austin and T. Negas, *J. Solid State Chem.*, 1980, **35**, 69.
32 J. E. H. Sansom, L. Hildebrandt and P. R. Slater, *Ionics*, 2002, **8**, 155.
33 J. R. Tolchard, J. E. H. Sansom, P. R. Slater and M. S. Islam, *J. Solid State Electrochem.*, 2004, **8**, 668.
34 E. J. Abram, C. A. Kirk, D. C. Sinclair and A. R. West, *Solid State Ionics*, 2005, **176**, 1941.
35 E. Kendrick and P. R. Slater, manuscript in preparation.
36 P. Berastegui, S. Hull, F. J. Garcia Garcia and J. Grins, *J. Solid State Chem.*, 2002, **168**, 294.
37 L. Leon-Reina, J. M. Porras-Vasquez, E. R. Losilla and M. A. G. Aranda, *J. Solid State Chem.*, 2007, **180**, 1250.